

## UNUSUAL X-RAY CHARACTERISTICS OF VERMICULITE FROM WIRY, LOWER SILESIA, POLAND

BORIS A. SAKHAROV<sup>1</sup>, ELŻBIETA DUBIŃSKA<sup>2</sup>, PAWEŁ BYLINA<sup>3</sup> AND GRZEGORZ KAPRON<sup>2</sup>

<sup>1</sup> Geological Institute, Russian Academy of Sciences, Pyzhevsky Street 7, 109017 Moscow, Russia

<sup>2</sup> Institute of Geochemistry, Mineralogy and Petrology, Faculty of Geology, Warsaw University, al. Żwirki i Wigury 93, 02–089 Warsaw, Poland

<sup>3</sup> Institute of Geological Sciences, Polish Academy of Sciences, ul. Twarda 51/55, 00–818 Warsaw, Poland

**Abstract**—Coarse-grained vermiculite from a serpentinite-pegmatite thermal zone displays a rational series of narrow 14.4 Å basal reflections and an unusual broad 28 Å peak. X-ray diffraction simulations and fitting techniques show that the 28 Å peak is related to 28 Å domains consisting of elongated 2:1 layers of different lengths. The domains are located at the crystal edges of the vermiculite.

**Key Words**—Crystal Edge, Interstratified Mineral, Vermiculite, XRD Characteristics.

### INTRODUCTION

The X-ray identification of vermiculite would appear to be simple: it is distinguishable from other clay minerals after undergoing various treatments (*e.g.* ethylene glycol,  $Mg^{2+}$  + glycerol, heating, and saturation with several exchangeable cations). However, spontaneous rehydration after heating and ambiguous results of swelling tests, primarily related to slow adsorption of ethylene glycol and glycerol, make unambiguous identification of vermiculite time consuming and difficult (MacEwan and Wilson, 1980; de la Calle and Suquet, 1988; Pons *et al.*, 1989; Reichenbach and Beyer, 1994, 1995; Reichenbach and Schütte, 1995; Moore and Reynolds, 1997). The diffraction patterns of regularly interstratified (Reichweite,  $R = 1$ ) minerals with vermiculite layers, *e.g.* high-charge corrensite and hydrobiotite, display strong low-angle superstructure peaks both in air-dried and ethylene glycol-treated samples. Nevertheless, the correct identification of expandable layers in the trioctahedral interstratified minerals may be problematic.

This study concerns a detailed analysis of unusual diffraction characteristics of vermiculite from Wiry, Lower Silesia, Poland. These features occur mainly on the low-angle diffraction peak. The vermiculite from Wiry is a product of phlogopite alteration, found in the contact zone between serpentinite and granite-type apophysis. Details of the vermiculite occurrence are given in Sachanbiński (1993), Jelitto *et al.* (1993), Dubińska *et al.* (1995), and Janeczek and Sachanbiński (1995).

### MATERIAL AND METHODS

Grain fractions were obtained by soaking the sample in double-distilled water until it disaggregated. Coarse flakes were separated using a nylon sieve (0.1 mm) and purified by hand, using a binocular microscope. Fine-grained fractions of the same sample were sepa-

rated using repeated centrifugal sedimentation in double-distilled water.

All X-ray diffraction (XRD) patterns were obtained on a DRON-1 diffractometer, using  $CoK\alpha$  radiation (Fe-filtered), 1.0 and 0.5 mm divergence slits, 0.25 mm receiving slit,  $0.04^\circ 2\theta$  steps, a counting time of 5 s per step, and a  $1.5\text{--}45^\circ 2\theta$  angular range. Oriented clay aggregates were prepared on 7 cm length glass slides by the pipette method using  $2.5\text{ mg/cm}^2$  of specimen. Samples were treated overnight with liquid ethylene glycol. The specimens were heated for 2 h on a home-made thermal stage and XRD patterns were recorded at temperatures of 75, 150 and  $250^\circ\text{C}$ . The XRD patterns of specimens heated at  $500^\circ\text{C}$  were recorded after cooling the specimen. The patterns were collected using the DRONEK software (W. Musiał, unpublished manuscript, 1992).

Simulated diffraction patterns of various structural models were calculated using the ASN program (Drits and Sakharov, 1976). The  $z$  atomic coordinates for different types of layers for simulations were obtained from Walker (1975) and Moore and Reynolds (1997). The instrumental factors recommended by Drits and Tchoubar (1990), *i.e.* sizes of the divergent and receiving slits, distances between X-ray source, sample and detector, and specimen size and thickness were used. The particle orientation factor,  $\sigma^*$ , of  $12^\circ$  (Reynolds, 1986) was also included in the calculations. The lognormal distribution of the thickness of the coherent scattering domain (CSD) was adopted (Drits *et al.*, 1998) to obtain the best fit between calculated and experimental curves. The authors changed the independent parameters for each calculated X-ray curve to accommodate  $d$ -values, intensity ratios, and profiles on experimental and simulated patterns.

The chemical composition of the sample studied (calculated on the basis of  $O_{10}(OH)_2$  per formula unit) is:  $Mg_{0.39}Ca_{0.01}(Mg_{2.73}Fe^{3+}_{0.27})(Si_{2.93}Al_{1.05}Fe^{3+}_{0.02})O_{10}(OH)_2$ , where  $Fe^{3+}$  is equal to total Fe on the basis of wet chem-

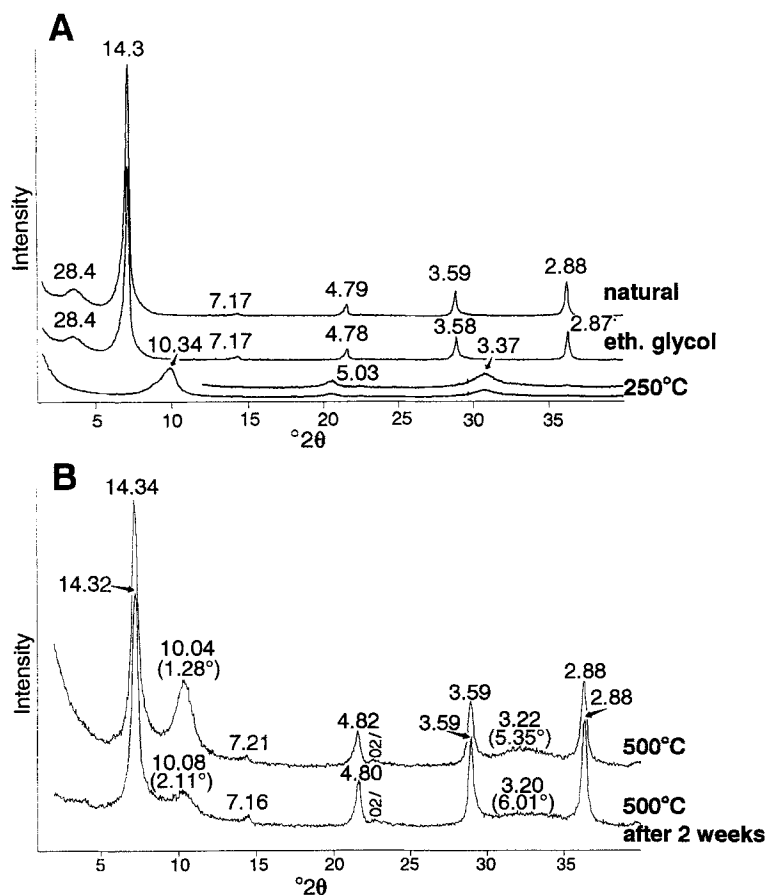


Figure 1. Experimental (observed) XRD patterns of a vermiculitic sample from Wiry, using oriented aggregate specimens. (A) Natural—air-dried specimen, eth. glycol—ethylene glycol-solvated specimen,  $250^{\circ}\text{C}$ —pattern recorded using a heating stage. The upper line represents an enlarged pattern. The sample was not completely anhydrous and it portrays an irregularly interstratified structure ( $R = 0$ ) composed of  $10.2$  Å layers (anhydrous vermiculite, 85 vol.%),  $11.6$  Å layers (one-layer  $\text{H}_2\text{O}$  complex of vermiculite, 7.5 vol.%) and  $14.4$  Å layers (two-layer  $\text{H}_2\text{O}$  complex of vermiculite, 7.5 vol.%). (B) XRD patterns of the specimen heated to  $500^{\circ}\text{C}$  in an oven, recorded immediately after cooling and two weeks later. The FWHM values are given in parentheses; the intensity of the  $\sim 14$  Å peak on the XRD pattern of heated specimen in (B) is  $\sim 5\times$  smaller than the corresponding peak of the untreated sample in (A);  $\text{CoK}\alpha$  radiation, grain fraction  $>0.1$  mm, flakes selected under binocular microscope.

ical analysis, *i.e.* using atomic absorption spectroscopy (AAS) for Si, Al, Ti, Fe, Mn, Ni, Cr, Zn and Cu and flame atomic emission spectroscopy (FAES) for Na, K, Ca, Li, Rb and Cs. For the analyses we used  $\text{HF}$ - or  $\text{HCl}$ -digested samples. We assumed that  $\text{Fe}^{3+}$  can be placed in tetrahedral sites to complete a total of 4.0 tetrahedral cations. Simulated XRD patterns were calculated using fixed element ratios.

## RESULTS AND DISCUSSION

The XRD pattern of the natural and glycolated coarse flakes shows a series of sharp  $00l$  reflections of typical vermiculite, and a broad low-angle band at  $\sim 28$  Å (Figure 1A). The reflection positions, intensities, and profiles are almost the same in both the natural and glycolated specimens. The  $28$  Å diffraction maximum was obtained at high relative humidity (r.h.

$> 80\%$ ). The maximum disappeared at low r.h. (10%) and only a rational series of  $14.3$  Å basal reflections of vermiculite were visible. This effect is reversible, *i.e.* the maximum appears again with increasing r.h.

The XRD pattern of the sample heated at  $500^{\circ}\text{C}$  and recorded after cooling the specimen (Figure 1B) reveals two series of peaks: (1)  $\sim 14.3$  Å (full width at half-maximum peak height, FWHM,  $0.4$ – $0.6^{\circ}2\theta$ ) and (2) two broad bands:  $\sim 10$  Å (FWHM at  $1.28^{\circ}2\theta$ ); and  $3.2$  Å (FWHM at  $5.35^{\circ}2\theta$  are presumably several broad and poorly resolved diffraction maxima). Both series are related to the unstable irregularly interstratified structures composed of common vermiculite and partly and/or fully dehydrated vermiculite. Rehydration occurred upon (or immediately after) cooling of the specimen. Our efforts to avoid spontaneous rehydration of the vermiculite by using conventional heating procedures failed.

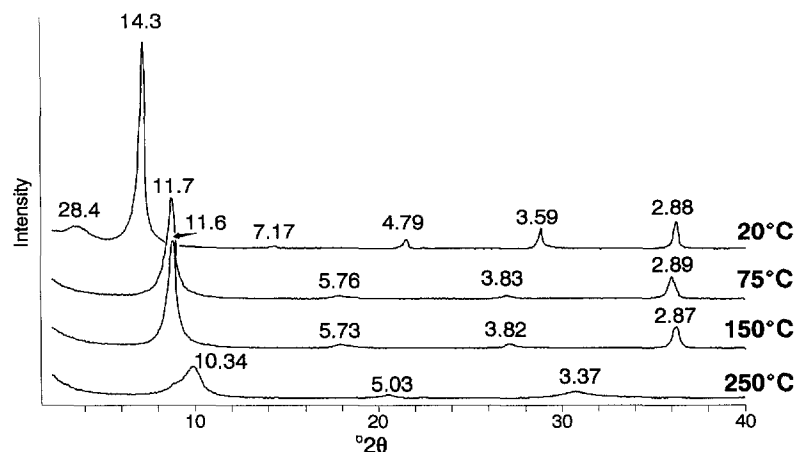


Figure 2. Experimental (observed) XRD patterns of a vermiculitic sample from Wiry (grain-size of  $>0.1$  mm, flakes selected under microscope) using oriented aggregate specimens. The traces were recorded after 1 h heating on a heating stage at each temperature.  $\text{CoK}\alpha$  radiation.

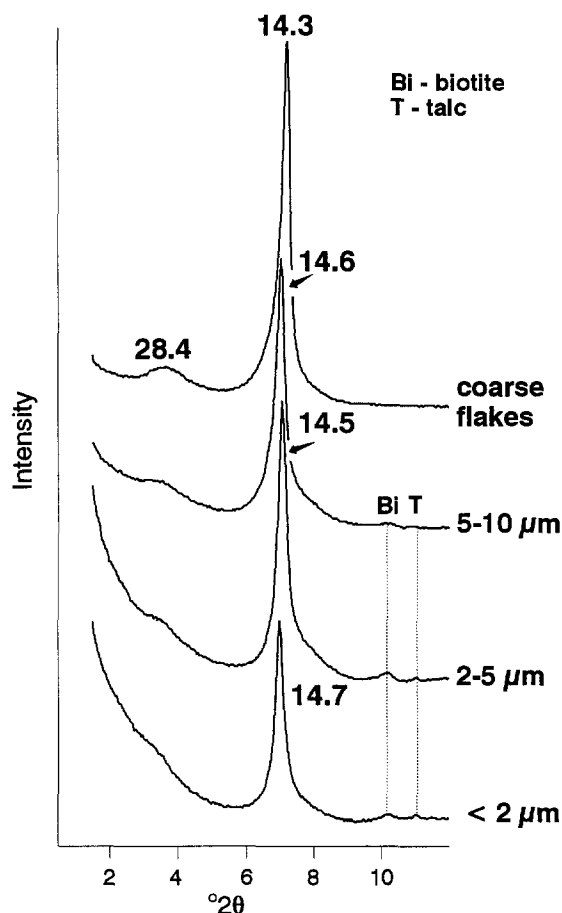


Figure 3. Experimental (observed) XRD patterns of different grain size-fractions (flakes  $>0.1$  mm, 5–10  $\mu\text{m}$ , 2–5  $\mu\text{m}$ ,  $<2$   $\mu\text{m}$ ) separated from a vermiculitic sample from Wiry. The intensity of 28 Å diffraction maxima decreases with decreasing grain size-fraction.  $\text{CoK}\alpha$  radiation.

Patterns obtained from heating the sample for 2 h at 75 and 150°C without cooling the specimen (Figure 2), show a nearly rational series of basal reflections with  $d(001) = 11.6\text{--}11.7$  Å, which indicates a single  $\text{H}_2\text{O}$  layer in partially dehydrated vermiculite interlayers. Similar heating procedures at 250°C produced an irrational series of basal maxima (Figure 2). These results generally agreed with Mg-exchanged vermiculite behavior under heating (cf. Collins *et al.* 1992; Reichenbach and Beyer, 1994; Ruiz-Conde *et al.*, 1996). Figure 3 shows X-ray patterns of different size-fractions of the studied sample. The intensity of the 28 Å peak diminishes gradually when obtained from coarse flakes or size fractions of  $<2$   $\mu\text{m}$ .

Several structural models may be suggested to explain the observed diffraction effects: (1) an interstratified structure; (2) a vermiculite-type structure composed of layers with an inhomogeneous distribution of 2:1 layers and/or interlayers; (3) a mixture of vermiculite and an interstratified mineral; and (4) a vermiculite structure with unusual crystal edges as described below. Each model was examined in detail by considering the position of peaks, intensities and profiles.

#### Interstratified structure models

*Interstratified vermiculite-chlorite*,  $R = 1$ . The calculated positions of diffraction peaks apparently fit well with experimental results of both the natural and glycolated samples. However, the brucite-like sheets should persist at moderate heating (250°C), whereas the vermiculite interlayers collapsed readily. Therefore, a regularly interstratified chlorite (14.2 Å)-dehydrated vermiculite (10 Å), *i.e.* 24 Å structure, should have been produced. Calculated X-ray patterns for this structure depart considerably from the observed patterns. Simulated X-ray patterns for structures with different ratios and/or different distribution of layer types

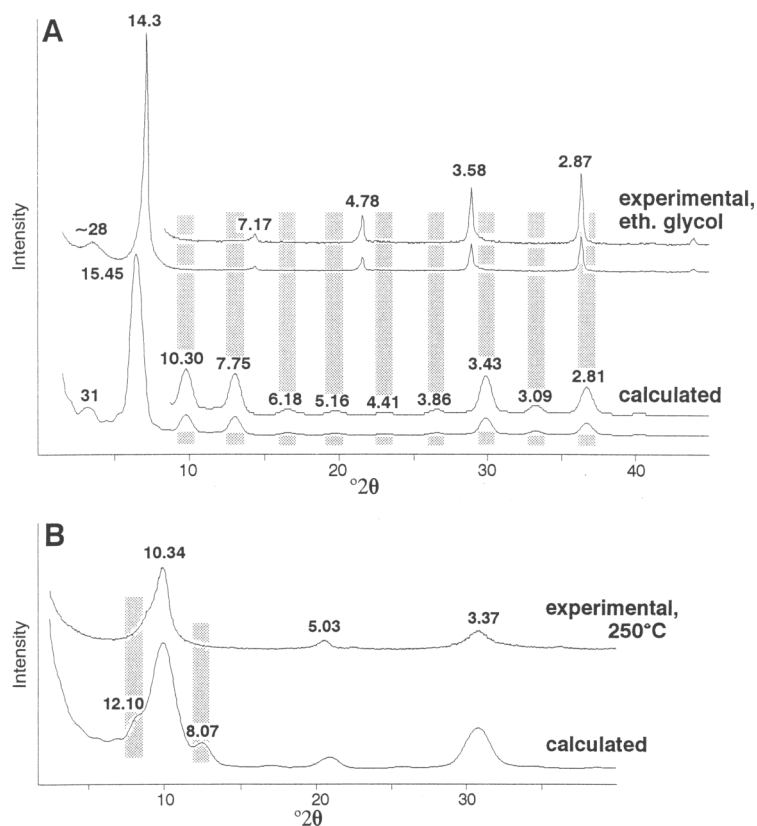


Figure 4. (A) Experimental (observed) XRD pattern of the coarse flake-fraction treated with ethylene glycol and a calculated regularly-interstratified vermiculite-saponite pattern, with  $R = 1$ . The vermiculite layers contain a single layer of glycol molecules, the saponite layers contain two layers of ethylene glycol, with the total Fe content located in saponite layers. (B) Experimental XRD pattern of the coarse flake-fraction heated to 250°C (heating stage) and a calculated pattern of the mixture composed of regularly interstratified chlorite-vermiculite (90 vol.%, vermiculite layers contracted) and regular vermiculite (10 vol.%, contracted layers). The gray bars represent reflections on calculated traces, absent from experimental patterns. CoK $\alpha$  radiation.

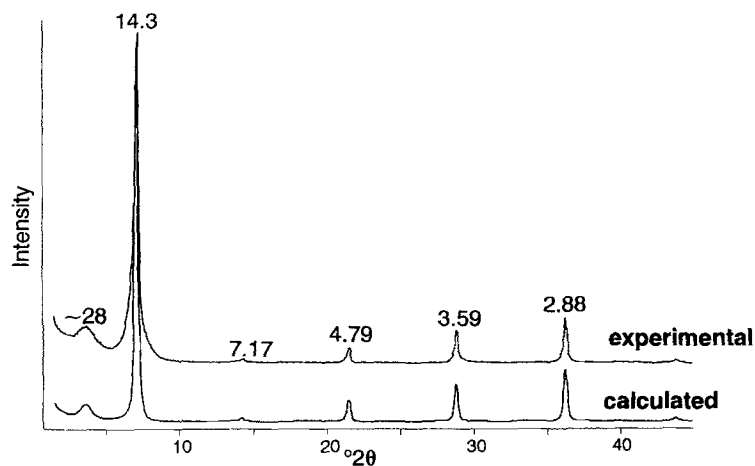


Figure 5. Calculated X-ray traces of vermiculite and unusual 28 Å domain. The calculated pattern represents a mixture of regular vermiculite (93 vol.%) and 28 Å edge layers (7 vol.%). CoK $\alpha$  radiation.

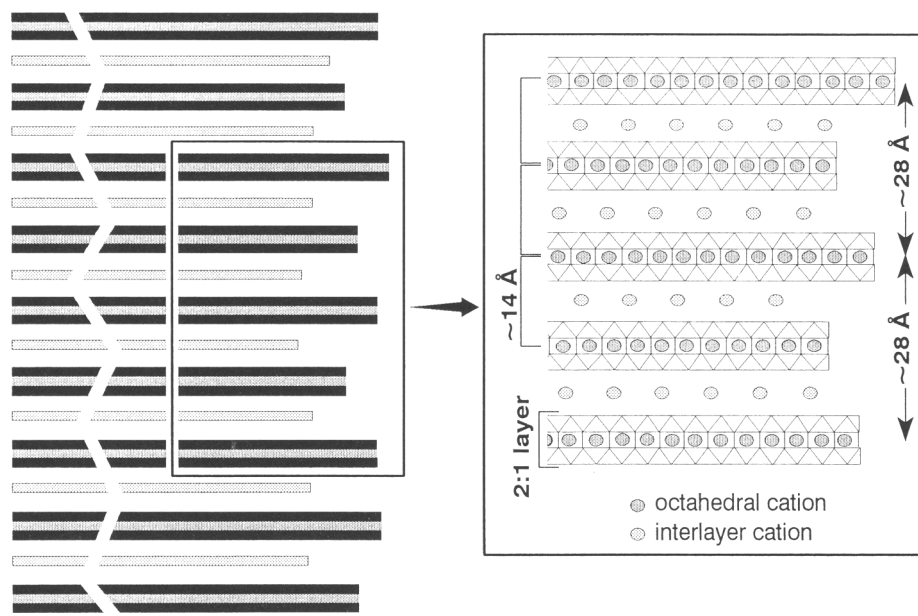


Figure 6. Model of vermiculite structure with 28 Å domains stable in high r.h. conditions.

showed that the 28 Å peak disappeared immediately when layer ratios were not equal to 1:1, or when the regularity of interstratification decreased.

*Interstratified vermiculite-smectite*,  $R = 1$ . Because observed X-ray tracings of the glycolated sample do not show swelling effects, there is no evidence sup-

porting an interstratified vermiculite-smectite model (Figure 4A). We considered several models of vermiculite-smectite interstratification, including different coherently scattering domain sizes and distributions and different locations of heavy cation and different numbers of octahedral vacancies. The results of these calculations were inconsistent with the observed patterns.

*Interstratified vermiculite-mica*,  $R = 1$ . Interstratified vermiculite-mica models must be rejected because the sample does not contain K, Na, or other elements that can be placed into a mica-like interlayer.

*Vermiculite-type mineral comprising layers with an inhomogeneous distribution of 2:1 layers and/or interlayers*

Inhomogeneity in vermiculite can result from: (1) different octahedral Fe content in adjacent layers; (2) polar 2:1 layers owing to different Al-Si substitution in the tetrahedral sheets and thus, different layer charge and interlayer cation and water contents; and (3) various interlayer cations and water contents with different positions.

These models were examined in detail. However, the resulting calculated patterns did not compare well with the observed XRD patterns. Although some calculated patterns show a 28 Å peak, these patterns always showed a relatively intense 9.6 Å peak; moreover, the observed 28 Å peak was broader than the calculated peak, whereas other calculated parts of the pattern fit well with the observed patterns. Thus, models involving inhomogeneity of vermiculite are rejected.

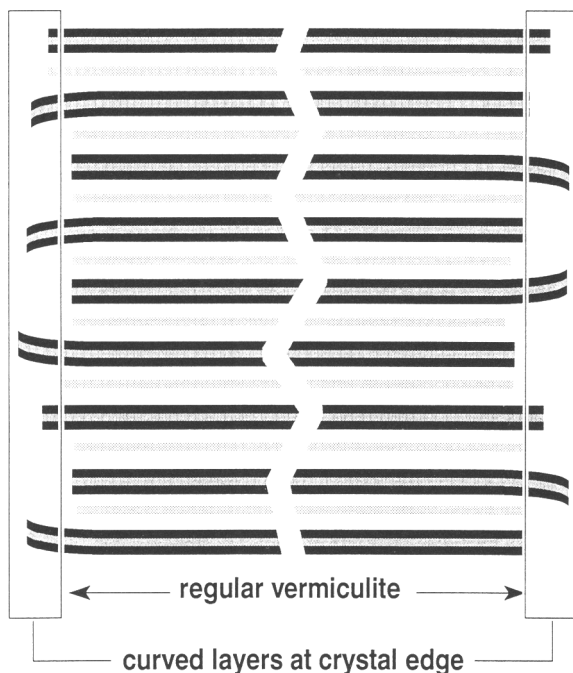


Figure 7. Model of 'ski-like' terminal edges of dehydrated domain.

### A mixture of vermiculite and interstratified mineral

The data observed can be interpreted tentatively as a mixture of vermiculite as the dominant phase with minor interstratified chlorite-vermiculite or inhomogeneous vermiculite. We examined these mixtures using fitting procedures for simulated and observed XRD patterns. All trials were unsuccessful. Figure 4B shows an example of a mixture composed of interstratified chlorite-vermiculite and vermiculite. The X-ray patterns of both untreated and glycolated samples can be accepted provisionally. However, heated corrensite produces an XRD pattern which differs from the observed pattern (Figure 4B).

A model of a mixture composed of Mg-exchanged vermiculite with a large CSD thickness and inhomogeneous vermiculite with relatively small CSD thickness produced both 28 Å and 9.6 Å peaks, but the latter peak was absent from the observed patterns.

### A vermiculite structure with unusual crystal domains

The models described above cannot explain the observed diffraction effects. The 28 Å reflection is also more prominent in the coarse-grained vermiculite (Figure 3). Therefore, we suggest that the observed XRD effects arise from different domains consisting of 2:1 layers with a periodicity of 14 and 28 Å. These domains scatter X-rays independently. The 14 Å domains represent normal vermiculite, whereas the 28 Å domains are composed of 2:1 layers with interlayers containing unidentified material which scatters X-rays incoherently. Figure 5 shows the agreement of X-ray patterns calculated on the basis of the proposed model and observed curves. The reflection positions, intensities and profiles fit well.

A reasonable explanation of the 28 Å domains is the following: vermiculite crystals have ordered alternating and variable elongated 2:1 layers with differences in length at the crystal edges. Thus, 28 Å domains can occur along with 14 Å layer stacking (Figure 6). The average thickness of the 14 Å and 28 Å domains is equal to 20 and 3 layers, respectively. An approximate content of the 28 Å edge layers is ~7% of the total vermiculite volume. The 28 Å domains appear to lose their periodicity in low humidity and during heating to produce a 'ski-like' pattern (Figure 7) similar to edges observed by Reichenbach *et al.* (1988) on high-resolution transmission electron microscope images.

## CONCLUSIONS

The X-ray pattern of Wiry vermiculite is unusual. The diffraction maximum at 28 Å is definitely not an artifact of instrumental parameters and was obtained only at exceptionally high relative humidity.

The vermiculite from Wiry is a transitional mineral in the sequence phlogopite → interstratified vermicu-

lite-phlogopite → vermiculite → saponite, where honeycomb saponite aggregates unequivocally form owing to dissolution-precipitation (Jelitto *et al.*, 1993; Dubińska *et al.*, 1995). The 28 Å domains may be where initial dissolution of the vermiculite occurs.

## ACKNOWLEDGMENTS

We thank Z. Jońca for performing the wet chemical analyses. We are grateful to J. Mościcki for flake separation. We thank W. Musiał for the DRONEK software. We also thank S. Tspursky for useful discussions, and D. McCarty, J. Walker, H. Graf von Reichenbach and S. Guggenheim for their helpful suggestions to improve this manuscript. This investigation was supported by State Committee for Scientific Research (KBN 6P04D 014 09) and the Russian Science Foundation.

## REFERENCES

- Collins, D.R., Fitch, A.N. and Catlow, R.A. (1992) Dehydration of vermiculites and montmorillonites: a time-resolved powder neutron diffraction study. *Journal of Materials Chemistry*, **2**, 865–873.
- de la Calle, C. and Suquet, H. (1988) Vermiculite. Pp. 455–496 in: *Hydrous Phyllosilicates (exclusive of micas)* (S.W. Bailey, editor). Reviews in Mineralogy, **19**, Mineralogical Society of America, Washington, D.C.
- Drits, V.A. and Sakharov, B.A. (1976) X-ray Structural Analysis of Mixed-layer Minerals. *Transactions of Academy of Sciences U.S.S.R.*, **295**, Moscow, 252 pp. (in Russian).
- Drits, V.A. and Tchoubar, C. (1990) *X-Ray Diffraction by Lamellar Structures. Theory and Application to Microdivided Silicates and Carbons*. Springer-Verlag, Berlin-Heidelberg-New York-London-Paris-Tokyo-Hong Kong-Barcelona, 371 pp.
- Drits, V.A., Eberl, D.D. and Środoń, J. (1998) XRD measurement of mean thickness, thickness distribution and strain for illite and illite/smectite crystallites by the Bertaut-Warren-Awerbach technique. *Clays and Clay Minerals*, **46**, 38–50.
- Dubińska, E., Jelitto, J. and Kozłowski, A. (1995) Origin and evolution of granite-serpentinite reaction zones at Wiry, Lower Silesia. *Acta Geologica Polonica*, **45**, 41–82.
- Janeczka, J. and Sachanbiński, M. (1995) New data on hybrid pegmatite in serpentinite from magnesite mine in Wiry (Lower Silesia). *Przegląd Geologiczny*, **53**, 777–782 (in Polish).
- Jelitto, J., Dubińska, E., Wiewióra A. and Bylina, P. (1993) Layer silicates from serpentinite-pegmatite contact (Wiry, Lower Silesia, Poland). *Clays and Clay Minerals*, **41**, 693–701.
- MacEwan, D.M.C. and Wilson, M.J. (1980) Interlayer and intercalation complexes of clay minerals. Pp. 197–248 in: *Crystal Structures of Clay Minerals and their X-ray Identification* (G.W. Brindley and G. Brown, editors). Monograph, **5**, Mineralogical Society, London.
- Moore, D.M. and Reynolds, R.C. (1997) *X-ray Diffraction and the Identification and Analysis of Clay Minerals*. Oxford University Press, Oxford-New York, 378 pp.
- Pons, C.H., Pozzuoli, A., Rausell-Colon, J.A. and de la Calle, C. (1989) Mécanisme de passage de l'état hydraté à une couche à l'état "zero couche" d'une vermiculite-Li de Santa-Olalla. *Clay Minerals*, **24**, 479–493.
- Reichenbach, H. Graf v., Wachsmuth, H. and Marcks C. (1988) Observations at the mica-vermiculite interface with HRTEM. *Colloid & Polymer Science*, **266**, 652–656.

- Reichenbach, H. Graf v. and Beyer, J. (1994) Dehydration and rehydration of vermiculites: I. Phlogopitic Mg-vermiculite. *Clay Minerals*, **29**, 327–340.
- Reichenbach, H. Graf v. and Beyer, J. (1995) Dehydration and rehydration of vermiculites: II. Phlogopitic Ca-vermiculite. *Clay Minerals*, **30**, 273–286.
- Reichenbach, H. Graf v. and Schütte, R. (1995)  $P_{H_2O}$ -T stability diagrams of hydrated vermiculites, Clays: Controlling the Environment. Pp. 235–239 in: *Proceedings of the 10th International Clay Conference Adelaide, Australia 1993*, (G.J. Churchman, R.W. Fitzpatrick and R. A. Eggleton, editors). CSIRO Publishing Melbourne, Australia.
- Reynolds, R.C. (1986) The Lorentz-polarization factor and preferred orientation in oriented clay aggregates. *Clays and Clay Minerals*, **34**, 359–367.
- Ruiz-Conde, A., Ruiz-Amil, A., Pérez-Rodríguez, J.L. and Sánchez-Soto, P.J. (1996) Dehydration-rehydration in magnesium vermiculite: Conversion from two-one and one-two water layer hydration states through the formation of interstratified phases. *Journal of Materials Chemistry*, **6**, 1557–1566.
- Sachanbiński, M. (1993) Talc and vermiculite occurrence in ultramafic rocks of the Ślęza ophiolite (Lower Silesia). *Acta Universitatis Wraclaviensis*, **1412**, 63–117 (in Polish).
- Walker, G.W. (1975) Vermiculites. Pp. 155–189 in: *Soil Components, Vol. 2: Inorganic Components* (J.E. Gieseking, editor). Springer, New York-Berlin-Heidelberg.
- E-mail of corresponding author: dubinska@geo.uw.edu.pl  
(Received 21 June 2000; accepted 12 November 2000; Ms. 462, A.E. Douglas K. McCarty)